# Contribution of GABAergic Inhibition to Receptive Field Structures of Monkey Inferior Temporal Neurons

Yi Wang[1,2,3], Ichiro Fujita[1,2,3], Hiroshi Tamura[1] and Yusuke Murayama[2]

[1]Division of Biophysical Engineering, Graduate School of Engineering Science, Osaka University, Toyonaka, Osaka 560-8531, [2]Department of Cognitive Neuroscience, Osaka University Medical School, Suita, Osaka 565-0871 and [3]Core Research for Evolutional Science and Technology (CREST), Japan Science and Technology Corporation, Toyonaka, Osaka 560-8531, Japan

**Receptive field (RF) structures of neurons in area TE of the monkey inferior temporal cortex were investigated under blockade of inhibition mediated by γ-aminobutyric acid (GABA). Bicuculline methiodide, a $GABA_A$ receptor antagonist, was microiontophoretically administered to TE neurons. Blockade of inhibition enhanced responses to a particular range of visual stimuli not only at the RF center, but also at the periphery of or outside RFs where the stimuli originally evoked little or no response, enlarging the RFs. The strongest responses under normal and disinhibited conditions occurred at the RF center in most neurons. The largest increase in responses, reflecting the strongest inhibitory input, usually occurred at the RF center, but in some neurons it occurred in the periphery. A neuron had a silent region within its RF where some stimuli effective at adjacent locations could not elicit responses even under blockade of inhibition. We suggest that (i) afferent information to individual TE neurons originates from a wide retinotopic region beyond their normal RF; (ii) the afferent convergence is not necessarily complete throughout a RF; and (iii) GABAergic inhibition contributes to the generation of RF structures of TE neurons.**

## Introduction

The neural processes that lead to visual perception and recognition of objects occur in the occipitotemporal pathway of the primate brain (Ungerleider and Mishkin, 1982; Goodale and Milner, 1992). The response selectivity of neurons for object features becomes gradually complex along this pathway. Meanwhile, the receptive field (RF), a part of the visual field from where a neuron receives information, increases in size. All early visual areas (V1, V2, V4 and TEO) of this pathway are organized in a retinotopic manner and represent the central and contralateral visual fields (Hubel and Wiesel, 1974; Gattass *et al.*, 1981, 1988; Boussaoud *et al.*, 1991). At the final stage, TE neurons have a large RF, almost always covering the fovea (the center of gaze), and most of the RFs extend into the ipsilateral field across the vertical meridian (Gross *et al.*, 1972; Desimone and Gross, 1979). TE neurons selectively respond to a complex object feature (Desimone *et al.*, 1984; Tanaka *et al.*, 1991; Fujita *et al.*, 1992). This response selectivity is largely maintained within their RFs (Schwartz *et al.*, 1983; Lueschow *et al.*, 1994; Tovee *et al.*, 1994; Ito *et al.*, 1995). The translation-invariant selectivity has been thought to underlie invariant recognition of visual objects across frontoparallel translation (Gross and Mishkin, 1977; Seacord *et al.*, 1979).

γ-Aminobutyric acid (GABA) is a major inhibitory neurotransmitter of the cerebral cortex. Earlier studies have shown that blockade of intracortical inhibition mediated by GABA reduces orientation, direction and length preferences of area 17 neurons in the cat visual cortex (Sillito, 1975, 1977; Sillito and Versiani, 1977; Tsumoto *et al.*, 1979). Recent studies also indicate that GABA-mediated inhibition is involved in the generation of orientation, direction and color selectivities of macaque V1 neurons (Sato *et al.*, 1994, 1995, 1996). In the cat areas 17 and 18, blockade of the inhibition changes RF subfield structures of neurons. During the blockade, On and Off subfields of simple cells in space and time and those of complex cells in time become less isolated or even completely superimposed (Sillito, 1975; Wolf *et al.*, 1986; Eysel *et al.*, 1994; Eysel and Shevelev, 1998; Pernberg *et al.*, 1998; Murthy and Humphrey, 1999; Frégnac and Shulz, 1999). In area 17, GABAergic inhibition contributes to neuronal sensitivity for cross-like figures (Shevelev *et al.*, 1998). In the rat, cat and macaque somatosensory cortex, blockade of GABAergic inhibition markedly increases the RF size of neurons (Dykes *et al.*, 1984; Alloway *et al.*, 1989; Alloway and Burton, 1991; Kyriazi *et al.*, 1996). In the macaque prefrontal cortex, disinhibition results in a loss of the spatial selectivity for the position of a visual object in most neurons or an enhancement of the selectivity in a small portion of neurons that are not tuned originally. The effects are observed in the sensory, mnemonic and motor phases of the oculomotor delayed response task (Rao *et al.*, 2000). Blockade of GABAergic inhibition also expands the representation fields of the body motor map in the rat primary motor cortex. Inactivation of GABAergic inhibition within the forelimb representation endowed the adjacent cortical area controlling the vibrissa movement with the ability to govern the forelimb movement (Jacobs and Donoghue, 1991). These results indicate that GABAergic inhibition plays important roles in the generation of RF properties of neurons in the primary sensory, motor, and higher-order association cortices.

In the macaque area TE, 25% of neurons are immunoreactive to antibodies raised against GABA or GABA-synthesizing enzymes, and are distributed throughout the cortical layers (Hendry *et al.*, 1987; Tanigawa *et al.*, 1998). Our recent study has shown that GABAergic inhibition is critically involved in the generation of selectivity of TE neurons to stimuli shown at the RF center (Wang *et al.*, 2000). In the present study, we presented stimuli at different locations within and outside RFs and investigated the role of GABAergic inhibition in the construction of the RF structures of TE neurons by microiontophoretically administering bicuculline methiodide, a $GABA_A$ receptor antagonist, to TE neurons. Stimulus selectivity of TE neurons was first identified by the 'reduction process', in which the stimulus feature critical for activation was determined by stepwise simplification of the most effective stimulus (Tanaka *et al.*, 1991; Fujita *et al.*, 1992; Kobatake and Tanaka, 1994). Then, visual responses of a TE neuron were tested by presenting stimuli at the RF center and four surrounding locations, or at seven locations along the horizontal dimension across its RF under normal and disinhibited conditions. The procedure enabled us to examine the contribution of GABAergic inhibitory input to the RF structures of the functionally characterized TE neurons.

## Materials and Methods

### *Animal Preparation and Surgical Procedure*

Two adult monkeys (*Macaca fuscata*), weighing 5.5 and 7.2 kg, were prepared for repeated recording experiments. The recording experiments were performed once a week on each monkey. All surgical and animal care procedures complied with the guidelines of the National Institutes of Health (1996), and were approved by the animal experiment committee of Osaka University Medical School.

For the preparatory aseptic surgery, the initial anesthesia was induced with ketamine hydrochloride (10 mg/kg, i.m.) after atropine sulfate (0.25 mg, i.m.) had been administered to the monkeys. Anesthesia was maintained with 35 mg/kg pentobarbital sodium (i.p.), supplemented at 5–10 mg/kg/h when necessary. The monkeys were placed on a stereotaxic apparatus. A plastic block for restraining the head was mounted to the skull with stainless steel or plastic screws and acrylic resin. The temporal part of the skull was exposed and covered with resin for subsequent unit recordings. The wound was infiltrated with a local anesthetic (xylocaine) during the surgery and treated with iodine and an antibiotic powder after the surgery. After the monkeys were allowed to recover from the surgery for >2 weeks, the optics of their eyes were checked under anesthesia to select appropriate contact lenses. The curvature of the cornea was first measured using a kerato-refractometer (Topcon, KR-7100, Japan). After a pair of transparent contact lenses with an appropriate curvature was placed on the corneas, the refractive power (diopter) of the eyes was measured. Then, photographs of the fundus of the eyes were taken with a retinal camera (Topcon, TRC-50X, Japan) to determine the positions of the optic disc and the fovea.

In the recording experiments, the monkeys were initially anesthetized with ketamine and atropine. An endotracheal cannula was inserted into the tracheal opening of each monkey. The monkeys were artificially respirated with a mixture of air and 1–2% isoflurane for the subsequent anesthesia. A small hole for electrode penetration was drilled in their skulls over the temporal cortex. During the recording sessions, the monkeys were immobilized with pancuronium bromide (0.02–0.04 mg/kg/h, i.v.), infused with physiological saline which contained 5% glucose and atropine sulfate (0.005 mg/kg/h, i.v.), and anesthesia was maintained with a mixture of $N_2O$ and $O_2$ (7:3) and 0.5–1.0% isoflurane. The electrocardiogram and expired $CO_2$ level (4.0–4.5%) were monitored throughout the duration of the experiment. Body temperature was maintained at 37–38°C. The pupils were dilated and the lenses were relaxed by local application of 0.5% tropicamide and 0.5% phenylephrine. The corneas were protected with contact lenses of appropriate refractive power and curvature with an artificial pupil (diameter 3 mm) to focus on a CRT monitor placed 57 cm away from the corneas.

After each recording session, the hole on the skull was cleaned with saline, treated with several drops of 8 mg/ml Decadron (dexamethasone sodium phosphate) on the dura and then covered with small pieces of aseptic medical sponges, antibiotic cream and resin. Within 1 h following the termination of pancuronium bromide, $N_2O$–$O_2$ and isoflurane administration, the monkeys recovered their spontaneous respiration to the normal level. Then, the artificial respiration was stopped. Before returning to their cage, the monkeys were injected with 0.5 mg Vagostigmin (neostigmine methylsulfate) to ensure recovery of their spontaneous respiration and then with an antibiotic. Each recording experiment lasted <16 h from the introduction of anesthesia to the recovery of spontaneous respiration of the monkeys.

### *Neuronal Recording and Visual Stimuli*

Recordings were performed in the dorsal part of area TE (A10–14) in the inferior temporal cortex. The position of each penetration was determined with reference to a marker placed on the resin-coated skull. In one monkey, electrode penetrations were guided by magnetic resonance imaging. Within the hole made in the skull over the temporal cortex, a pinhole was made in the dura using a stainless steel needle with a shaft 0.7 mm in diameter. Then a triple-barreled, glass-coated tungsten microelectrode (see below) was inserted into the cortex through the pinhole using a conventional microdriver. The exposed dura was covered with wax to prevent it from drying and to reduce movement of the cortex caused by pulsation and ventilation. Extracellular action potentials were recorded from single TE neurons and amplified by conventional techniques. Action potentials from single neurons were isolated based on their wave form and amplitude using a window discriminator. Only neurons that were well isolated from other neurons and the background noise were used for the present analysis. The timing of action potentials was recorded using a computer with 1 ms resolution.

After neuronal activity from a single neuron was isolated, we determined its stimulus selectivity. Visual stimuli were presented to the eye contralateral to the recorded hemisphere. Visual responses of a neuron were first tested using >90 hand-held real objects and many two-dimensional paper cutouts to search for effective stimuli. Images of effective stimuli were then obtained with a video camera and modified on a computer. Images of these stimuli were presented on a CRT monitor. The critical stimulus feature essential for activation of a neuron was determined by stepwise simplification of the most effective stimulus, i.e. the 'reduction process' (Tanaka *et al*., 1991; Fujita *et al*., 1992; Kobatake and Tanaka, 1994). We then selected the most effective and simplest stimulus and two other effective or ineffective stimuli for analysis of RFs.

For each neuron tested, the position and size of the RF were first explored by presenting the selected stimuli at the center and four surrounding locations of a region covering the central part of the visual field. Based on responses obtained at the five locations, we adjusted the central position of the CRT monitor to the visual field where the strongest responses had been evoked. The responses of the neuron were again tested at the five locations to estimate the size and the center position of the RF. We then carried out the following experiments.

In one series of experiments, the stimuli were presented at the center and four surrounding locations covering the visual field of 7.5–17.5° × 7.5–17.5°. The covered area depended on the size of the preliminarily determined RF. When visual stimulation at the surrounding locations could not elicit responses even during application of bicuculline (see below), the surrounding stimuli were presented closer to the RF center and the responses of the neuron were tested again. The central location of the stimulus presentation corresponded to the center of the RF predetermined for each neuron. Thus, the central location of the stimulation was not always at the fovea of the visual field, because the RF centers of TE neurons were usually off from the fovea. Hereafter, when we mention 'ipsilateral' or 'contralateral' sides of RFs, this is with respect to the RF center and not with respect to the fovea.

In order to evaluate more quantitatively the effects of blocking GABAergic inhibition on the size and structure of RFs, we designed another series of experiments. Visual stimuli were presented at seven positions spanning 40° with a regular horizontal interval (6.7°) and the central stimulus location corresponded to the center of the predetermined RF.

In both series of experiments, stimuli were ~2.5° × 2.5° in size. The darkest luminance of the stimuli was 0.7 cd/m$^2$ and the brightest was 99.2 cd/m$^2$. The stimuli were presented for 1 s at non-overlapping local regions with a small-amplitude motion (up to 0.5°) on a gray background (15.7 cd/m$^2$). The time interval between two stimulus presentations was 1.5 or 2 s and each stimulus was presented 10 times. Because only a small number of the stimuli were used and TE neurons become habituated to a visual stimulus presented repeatedly at a short interstimulus interval (Gross *et al*., 1972; Miller *et al*., 1991), successive presentation of the same stimulus, even at different locations, was avoided in these experiments. Otherwise, the sequence of the stimuli was pseudorandom.

### *Microiontophoresis*

Triple-barreled microelectrodes were constructed as described elsewhere (Takao *et al*., 2000). One of the two glass barrels was filled with 2.5 or 5 mM bicuculline methiodide (pH 3.5, adjusted with HCl; Sigma) and the other with 0.9% NaCl (vehicle, pH 3.5). A low-intensity current (+1 to 5 nA) was used to eject a minimal amount of bicuculline to the immediate vicinity of the recorded neurons. Occasionally, bicuculline application caused epileptiform activity in the recorded neurons. In such cases, we decreased the ejection current until the activity disappeared. Otherwise, the recording was not performed at these sites. In most cases, the low-intensity current used (+1 to 5 nA) did not result in epileptiform activity. When bicuculline was not administered, a retaining current of −20 nA was employed to prevent leakage of bicuculline. Under all conditions, a balancing current with the same intensity and opposite polarity was applied to the vehicle barrel to offset possible current effects

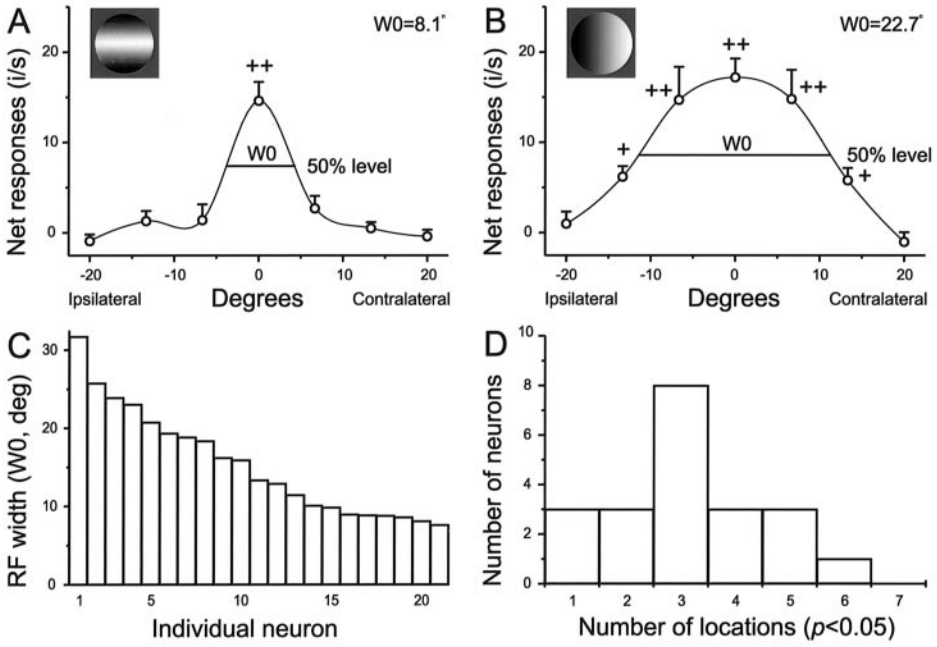


**Figure 1.** RFs of TE neurons under normal conditions. (*A*,*B*) RF tuning curves of examples of neurons with a small (*A*) and a large RF (*B*). The most effective stimuli are shown at the top left of each panel. Data points of responses tested at seven locations along the horizontal dimension were interpolated by cubic interpolation and the width of RF tuning curves (W0) was measured at the half-magnitude of peak responses (50% level). Abbreviation: i/s, impulses/s. +, ++: $P < 0.05$ or 0.01, *t*-test, relative to the spontaneous firing rate. Ipsilateral, contralateral: the ipsilateral or contralateral sides of an RF of the studied neuron with respect to the RF center and not the fovea of the visual field. Vertical bars: SEM. (*C*) Distribution of half-peak widths of RF tuning curves in 21 neurons to the most effective stimuli. (*D*) Distribution of RF sizes of the 21 neurons expressed as the number of locations where the most effective stimuli elicited statistically significant responses ($P < 0.05$, *t*-test; e.g. cell A had one and cell B had five locations).

on the recorded neurons. When the current polarity of the bicuculline barrel was reversed, the current polarity of the vehicle barrel was automatically reversed. We recorded responses of the neurons to the stimulus sets before, during and after bicuculline application. Usually, the effects of bicuculline on visual responses were tested after bicuculline had been applied for 5 min and recovery data were collected at least 5–10 min after bicuculline application was stopped. The electrodes allowed us to obtain single-unit recordings with a high signal-to-noise ratio and to maintain the single-unit recording for a sufficient time to finish three sessions before, during and after the bicuculline application. Usually, the entire process of examining a neuron, including the determination of its stimulus selectivity by the reduction process, took >2 h.

### *Data Analyses*

Firing rates of visual responses during 1 s of stimulus presentation were averaged from 10 presentations. Net visual responses were obtained by subtracting the spontaneous firing rate, which was measured during the 0.5 s prior to the presentation of each stimulus, from the visual response rate. A two-way analysis of variance (ANOVA, stimulated location versus drug condition) was applied to the net firing rates evoked by a stimulus before and during bicuculline application to detect effects of bicuculline on the RF of a neuron. We considered that bicuculline affected the RF if the responses to one of the stimuli used were significantly affected by bicuculline (Drug factor or Drug × Location interaction, $P < 0.05$). The ANOVA was also applied to the net firing rates before and after bicuculline application to assess whether a neuron recovers its original RF profile from the effects of bicuculline. We considered that a neuron had recovered from the effects of bicuculline if the responses to the stimulus between before and after bicuculline application were not significantly different (both Drug factor and Drug × Location interaction, $P > 0.05$). In order to examine interaction between bicuculline application and visual stimuli on RF structures, a three-way ANOVA with stimulus, location and drug as factors was applied to the net firing rates for each neuron.

A *t*-test was used to examine whether a stimulus evoked significant responses at a location relative to the spontaneous firing rate and also whether bicuculline significantly enhanced net responses at a location during bicuculline application in comparison with those before bicuculline application. Net responses at seven locations along the horizontal dimension were plotted against the horizontal positions and interpolated by cubic interpolation (MatLab), in which the interpolated curve passed through each of the original data points. Hereafter, we refer to the interpolated curve as an 'RF tuning curve'. The width of an RF tuning curve was measured at the half-magnitude level of the peak responses (see below for more details). For all the statistical tests, the significance level was $P < 0.05$.

## Results

We examined the effects of bicuculline on the RFs of 38 single TE neurons recorded from three hemispheres of two adult monkeys. The preferred stimuli of all these 38 neurons were determined by the 'reduction process' (see Materials and Methods). Of the 38 neurons, 17 were tested using stimuli presented at the RF center and four surrounding locations, which were at the periphery of the RF for some neurons or outside the RF for others. The remaining 21 were tested at seven locations along the horizontal dimension across their RFs.

### *RFs under Normal Conditions*

The RF size of the TE neurons under normal conditions (i.e. in the absence of bicuculline) exhibited a considerable extent of variation (Fig. 1). Some neurons responded to the most effective stimulus only at one location, while others responded to the stimulus presented at surrounding locations 20° away from the RF center. The neuron shown in Figure 1*A*, for example, responded strongly to a luminance gradation pattern presented at the center (0°), but showed very weak or no responses to the stimulus presented at locations >6.7° from the center. The width of the RF tuning curve measured at the half-magnitude of the peak response (W0) was 8.1°. Another neuron (Fig. 1*B*) respon-

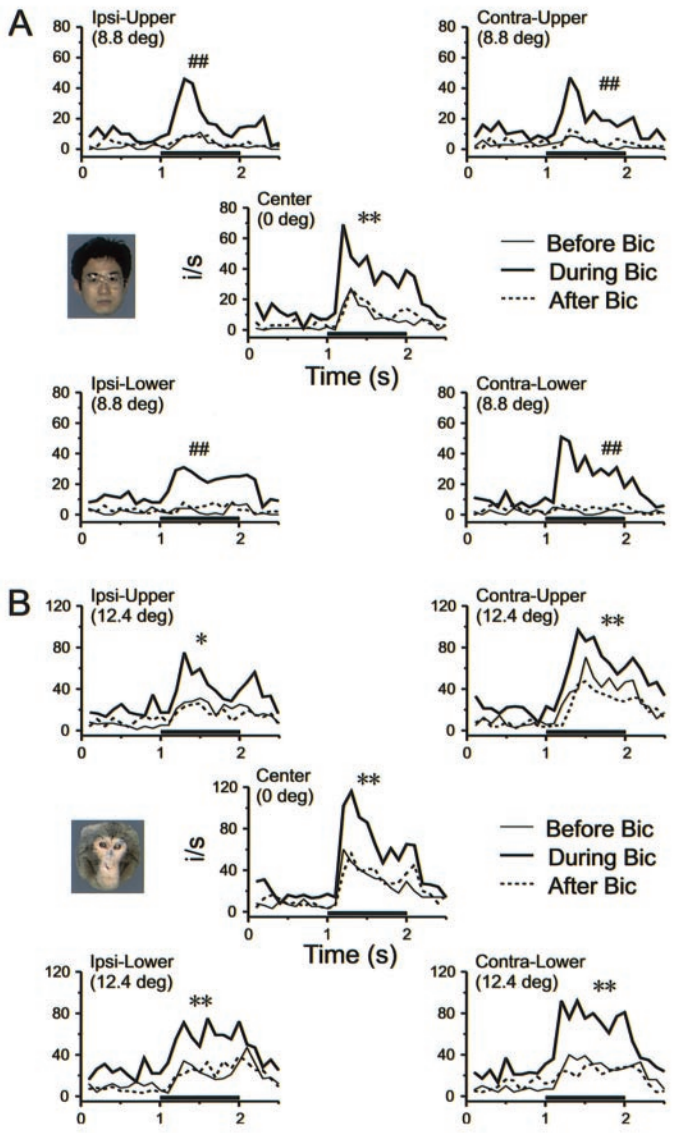


**Figure 2.** Effects of blocking GABAergic inhibition on visual responses of two neurons examined at the center and four surrounding locations. The two neurons were recorded 515 μm apart along one penetration vertical to the surface of the cortex, with a relatively small (*A*) and a large RF (*B*). Bin width of the peristimulus time histogram (PSTH) is 100 ms. Horizontal bar at the bottom of each PSTH indicates 1 s period of stimulus presentation. The faces shown are the most effective stimuli for respective neurons. *##*, *t*-test, relative to the spontaneous firing rate, $P < 0.01$ during bicuculline application and $P > 0.05$ before bicuculline application. **, *, $P < 0.01$ or 0.05, *t*-test for comparing net responses during bicuculline application with those before bicuculline application. Ipsi-, Contra-, the ipsilateral and contralateral sides of an RF with respect to the RF center and not the fovea. Upper, Lower, the upper or lower parts of an RF. The numbers in the left upper corner of these PSTHs indicate the distance from the RF center (0°). Before, during and after Bic, the responses obtained before, during and after bicuculline application, respectively.

ded to a different pattern of luminance gradation presented at five locations spanning 26.7°. The W0 of this neuron was 22.7°. The half-peak width of RFs among the 21 neurons tested at seven locations ranged from 7.6° to 31.7° (15.4 ± 6.9°, mean ± SD, Fig. 1*C*). The number of locations where the most effective stimulus evoked significant responses in a neuron was 3.1 ± 1.4 on the average (± SD, Fig. 1*D*). Seventy-one per cent of these neurons (15/21) responded to those presented at three or more locations. Only one of the 21 neurons responded at six locations (Fig. 1*D*); hence, the stimulated range (40°) in the seven-location experiments covered the entire RF of most of the studied neurons in the horizontal dimension. Most RF tuning curves were symmetrical approximately at the RF center under normal conditions (Figs 1*A*,*B* and 4). A few neurons (two of 21) exhibited an asymmetric RF tuning profile.

### *Effects of Bicuculline on RF*

Bicuculline affected the visual responses in 16 of the 17 neurons tested at five locations and in 20 of the 21 neurons tested at seven locations (ANOVA, Drug factor and/or Drug × Location interaction, $P < 0.05$). All of these neurons recovered from the effects after the application of bicuculline was stopped (both Drug factor and Drug × Location interaction, $P > 0.05$). The following analyses were based on the data of the 16 and 20 neurons.

#### *Five-location Experiments*

Bicuculline markedly enhanced responses of neurons to stimuli presented not only at the RF center as we showed in our previous study (Wang *et al.*, 2000), but also at the peripheral locations, where the stimuli originally evoked weak or no visual responses. Figure 2 shows the effects of bicuculline on responses of two neurons. They were recorded from two nearby sites along a vertical penetration and both responded preferentially to faces. The first neuron (Fig. 2*A*) originally responded to a human face presented only at the RF center. Following bicuculline application, it became responsive ($P < 0.01$) to the face at the four surrounding locations outside its original RF (8.8° from the center) as well as significantly increasing its responses at the center. This effect was observed only for the face stimulus, not for the other two stimuli, a concentric circle and a horizontal bar ($P > 0.05$). The second neuron with a large RF (>24.8°) significantly augmented its responses to a monkey face at the center and all four peripheral locations (12.4° from the center, Fig. 2*B*). This neuron also became responsive to a human face (for image, see Fig. 2*A*), which was ineffective across its large RF before bicuculline application ($P > 0.05$), at the left two surrounding locations (not shown; $P < 0.05$). These effects did not, however, occur in the responses to a horizontal bar ($P > 0.05$).

Figure 3 summarizes the effects of bicuculline on responses of the 16 neurons to their respective most effective stimulus. For the five neurons with small-size RFs tested at 5.3° (Fig. 3*A*), the average response at the four surrounding locations during bicuculline application was 458 ± 168% (±SD) of the original responses, while that at the center was 146% of the original response. For the seven neurons with middle-size RFs tested at 8.8° (Fig. 3*B*), the two values were 318 ± 53% and 248%; for the four neurons with large-size RFs tested at 12.4° (Fig. 3*C*), the two values were 226 ± 50% and 183%, respectively. The data demonstrate considerable effects of blocking of GABAergic inhibition on responses of TE neurons throughout their RFs (but see Fig. 10).

#### *Seven-location Experiments*

Data obtained from the 20 neurons in the seven-location experiments provided a quantitative assessment of the effects of bicuculline on the size and structures of the RFs. The effects were evaluated using two parameters: gain index and width of the RF tuning curves. The gain index (GI) is defined as (Ad – Ab)/Ab, where Ad and Ab are the areas (spikes/s × degrees) under the RF tuning curves during and before bicuculline application (see Fig. 5*E*), respectively. The unit of the index indicates that the area under an RF tuning curve during bicuculline

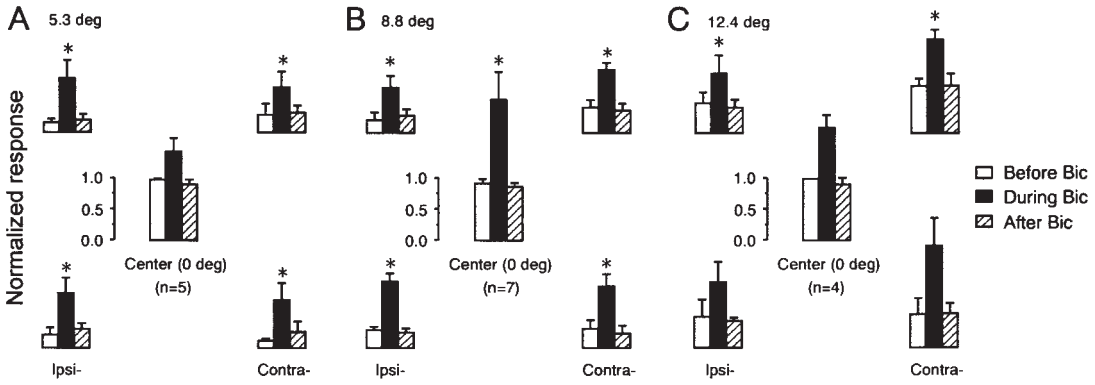


**Figure 3.** Summary data of 16 neurons tested in five-location experiments. Responses of neurons with small (*A*, $n = 5$), medium (*B*, $n = 7$) and large RFs (*C*, $n = 4$) to the most effective stimuli presented at the RF center and four surrounding locations 5.3° (*A*), 8.8° (*B*) and 12.4° (*C*) from the RF center. Net responses for each neuron before (open bars), during (filled bars) and after bicuculline application (hatched bars) were normalized with respect to the strongest ones at one of the five locations before bicuculline application. $*P < 0.05$, paired *t*-test for comparing net responses of these neurons during bicuculline application with those before bicuculline application. Vertical bars: SD.

application is increased by 100% from that before bicuculline application. The width of the RF tuning curve was measured at the half-magnitude of peak responses before (W0) or during (W1) bicuculline application, respectively. We also measured the width of the RF tuning curve during bicuculline application at the half-magnitude of the original peak responses (W2, see Fig. 5*E*).

Figure 4 shows five examples of neurons, the RFs of which were affected by bicuculline in different ways. The first neuron had a small RF to the most effective stimulus, a luminance gradation pattern (W0 = 7.6°, Fig. 4*Aa*). Bicuculline increased the area under the RF tuning curve by 200% (GI = 2.03). The half-peak width was broadened by 2.4° when the width before bicuculline application was compared with that during bicuculline application at the respective half-peak levels (ΔW1 = W1 – W0, Fig. 5*E*). When the widths of the RFs before and during bicuculline application were compared at the same original half-peak level, the change in the RF width was 8.7° (ΔW2 = W2 – W0, Fig. 5*E*). A plot of the normalized responses indicates that the RF profile of this neuron actually became broader following bicuculline application (Fig. 4*Ab*). The second neuron responded best to a black cross and had a large RF under normal conditions (W0 = 25.8°, Fig. 4*Ba*). The area under the RF tuning curve was doubled (GI = 1.08). The width was broadened by 13° at the original half-peak level (ΔW2), although the overall shape of the RF profile of the neuron was not changed (ΔW1 = 0.2°, Fig. 4*Bb*). Figure 4*Ca* shows that responses of a neuron to a cross of white outline were increased mainly at the RF central region. The GI was 0.71 for this neuron. The neuron had a large RF (W0 = 23.2°) and the width at the original half-peak level became larger by 3.5° (W2), whereas the change at the respective half-peak levels was –5.3° (ΔW1). The overall shape of its RF tuning curve became sharper in comparison with that before bicuculline application (Fig. 4*Cb*). The responses of the fourth neuron to a luminance contrast pattern were augmented mainly at the contralateral side of the RF (Fig. 4*Da*,*b*; for the definition of 'contralateral', see Materials and Methods). The half-peak width of the RF was increased by 11.9° (ΔW1) and the width measured at the original half-peak level by 17.3° (ΔW2). The neuron had a GI of 1.35. The fifth neuron had significantly enhanced responses to a red circle at both sides of the peak, but not at the peak (Fig. 4*E*). The half-peak width was increased by 9.3° (ΔW1) with a GI of 0.75. The overall RF was markedly broadened at both sides (ΔW2 = 9.2°, Fig. 4*Eb*). The results indicate that bicuculline enlarged the RFs of most neurons and also altered the shape of the RF tuning curve in many of them.

As shown in Figure 4, bicuculline shifted upward the entire or part of the RF tuning curves in individual neurons. Figure 5*A* shows the distribution of GIs for 47 RFs, which were tested using three stimuli for each of the 20 neurons and were affected by bicuculline (ANOVA, Drug factor and/or Drug × Location interaction, $P < 0.05$). The minimal and maximal GIs were 0.36 and 5.16, respectively. Eight-five per cent (40/47) of the RFs had a GI > 0.5 (e.g. the RFs in Fig. 4*C*,*E*) and 51% of the RFs (24/47) had a GI > 1 (e.g. the RFs in Fig. 4*A*,*B*,*D*). On average, the area under the RF tuning curve during bicuculline application was increased by 150% (GI = 1.47 ± 1.24, mean ± SD).

The change in the size of RFs was first assessed based on a change in the number of locations where a stimulus elicited significant responses of a neuron. The three neurons shown in Figure 4*A*,*D*,*E*, for example, originally responded to their preferred stimuli only at one location (RF center). Following bicuculline application, all of these neurons responded at three locations ($P < 0.05$). The distribution of the number of effective locations for the 47 RFs analysed in the 20 neurons was shifted by bicuculline toward larger values than that before bicuculline application (Mann–Whitney's *U*-test, $P < 0.01$; Fig. 5*B*). On average, the neurons responded at 2.4 ± 1.5 (mean ± SD) locations before bicuculline application and at 3.3 ± 1.5 locations during bicuculline application.

The change in the size of RFs was also evaluated as a change in the width of RF tuning curves. Figure 5*C* shows the effects of bicuculline on the width of 43 RF profiles that had a clear response peak both before and during bicuculline application among the 47 RFs. The three RFs in which neurons showed no visual responses (e.g. the RF of Fig. 8*B*) before bicuculline application and one RF in which a neuron had significant but weak responses (<5 spikes/s) at several locations before bicuculline application were excluded from the analysis. The width at the original half-peak level was increased from 14.1 ± 6.1° before bicuculline application (W0) to 22.4 ± 8.2° during bicuculline application (W2) (mean ± SD, $n = 43$). The change was significant (*U*-test, $P < 0.0001$, Fig. 5*C*).

We also compared the width of RFs between before (W0) and during bicuculline application (W1) at their respective half-peak levels. In the normalized plots of the RF tuning curves shown in Figure 4*Ab–Eb*, a difference between the two values (ΔW1 = W0 – W1) reflects a change in the shape of the RF tuning curve. For

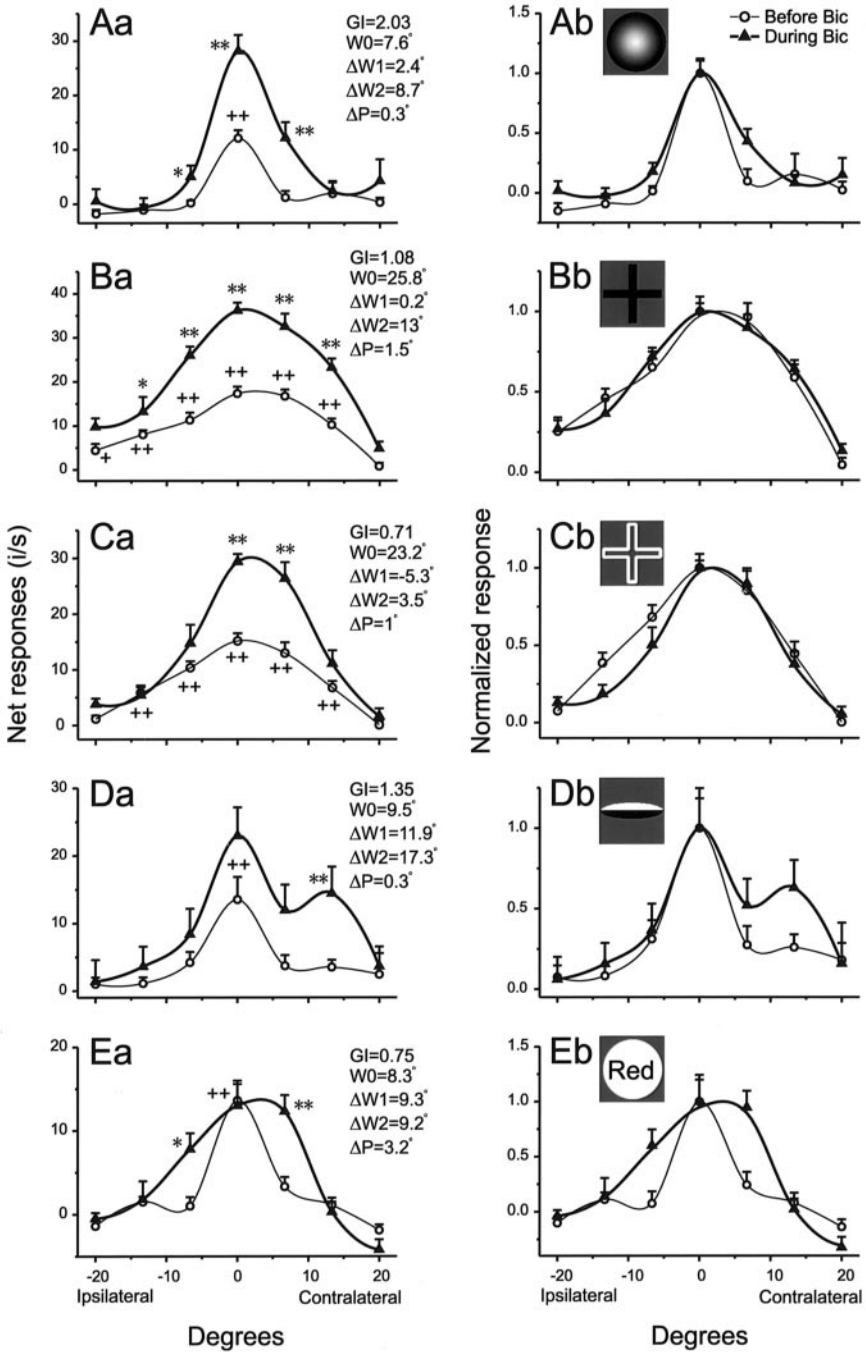


**Figure 4.** Effects of bicuculline on RF tuning curves of five neurons. Left panels (*Aa–Ea*) shown in net firing rates and right panels (*Ab–Eb*) in responses normalized with respect to the strongest responses before and during bicuculline application, respectively. (*Aa*) A neuron became responsive at both flanks outside its originally small RF. (*Ba*) Responses of a neuron were enhanced throughout its large RF. (*Ca*) Responses of a neuron were increased mainly in the central region of its large RF. (*Da*) Responses of a neuron were enhanced significantly at the contralateral side of the RF, but not at the ipsilateral side. (*Ea*) Responses of a neuron were augmented significantly at both sides of the response peak, but not at the RF center. The stimuli used are shown for each neuron. The filled triangles with thick lines and open circles with thin lines represent the data during and before bicuculline application, respectively. GI, gain index (see Fig. 5 caption); ΔW1, difference of the widths of RF tuning curves between before (W0) and during bicuculline application (W1) measured at the respective half-peak levels (W1 – W0); ΔW2, difference of the widths of RF tuning curves between before (W0) and during bicuculline application (W2), measured both at the original half-peak level (W2 – W0), i.e. before bicuculline application; ΔP, change in the position of the response peak before and during bicuculline application. For W0, W1 and W2, see Figure 5*E*. For other conventions, see Figures 1 and 2.

35% of the RFs (15/43, Fig. 5*D*), the difference was >2°. The shape of these RFs became broader during bicuculline application than before bicuculline application (e.g. the RFs in Fig. 4*A*,*D*,*E*), due to a larger amount of disinhibition at the RF periphery. For the other 21% of the RFs (9/43), the difference was <–2° (ΔW1) and their shape became sharper, due to a higher disinhibition at the RF center than at the periphery (e.g. the RF in Fig. 4*C*). The shape of the remaining 44% (19/43) of the RFs did not obviously change during bicuculline application (–2° ≤ ΔW1 ≤ 2°, e.g. the RF in Fig. 4*B*). For these RFs, the degree of

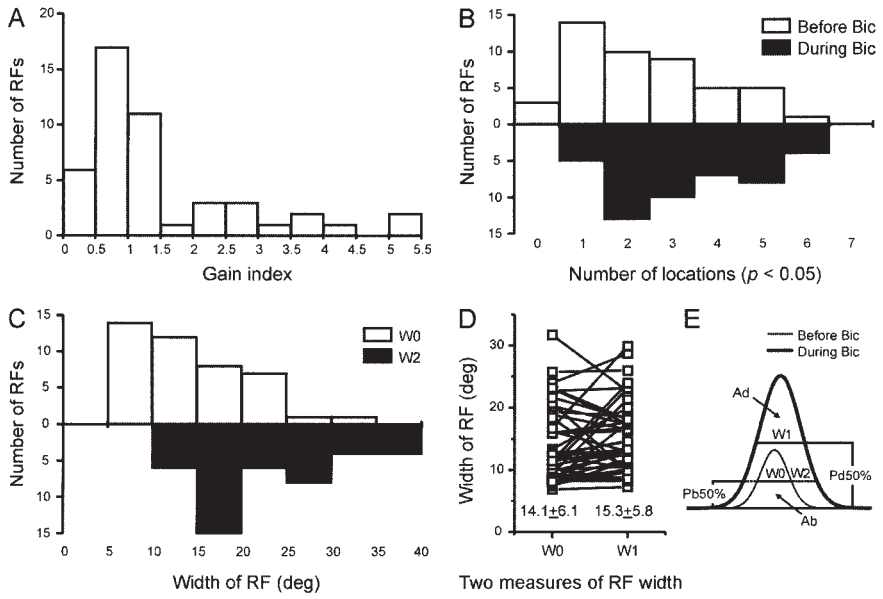


**Figure 5.** Blockade of GABAergic inhibition enlarged the RF (*A–C*) and altered its shape (*D*). (*A*) Distribution of gain indices of 47 RFs. Gain index = (Ad – Ab)/Ab, where Ab and Ad denote the areas below RF tuning curves before or during bicuculline application within the 40° or within the intersections of the curves with the base line. (*B*) Distribution of the number of locations where a stimulus evoked visual responses ($P < 0.05$) before (open bars) and during bicuculline application (filled bars). The data are based on 47 RFs. (*C*) Distribution of the width of RF tuning curves ($n = 43$) at the original half-peak level. W0, before (open bars); W2, during bicuculline application (filled bars). (*D*) Squares joined by a line indicate widths of each RF measured before (W0) and during bicuculline application (W1) at the respective half-peak levels. The numbers below the plot indicate means ± SD of the widths. (*E*) The figure shows how the widths of one-dimensional RF profile were measured; Pb50% and Pd50%, 50% magnitudes of peak responses before (thin curve) and during bicuculline application (thick curve), respectively; W0, RF width before bicuculline application at Pb50% level; W1, RF width during bicuculline application at Pd50% level; W2, RF width during bicuculline application at Pb50%.

disinhibition at the RF center and periphery during bicuculline application was approximately in proportion to the original response magnitudes at each location before bicuculline application. Thus the disinhibition altered the shape of the RF tuning curve in 56% of the RFs (24/43), suggesting that structures of these RFs were under the influence of GABAergic inhibition.

The effects of bicuculline on RF structures showed a considerable variation among the neurons (Figs 2–5). The change in the width at the original half-peak level (ΔW2 = W0 – W2, Fig. 5*C*), for example, ranged from –1.8 to 23.6°. The difference in the effects on the size of RFs may depend on the amount of bicuculline applied. A larger amount of effectively expelled bicuculline would remove a larger amount of inhibition and could affect RFs to a greater extent. To examine this possibility, we analysed the relationship between the change in ΔW2 and the change in the response magnitude at the original peak. We assumed that the latter is indicative of the amount of disinhibition, i.e. the amount of bicuculline applied. The change in the half-peak width was not correlated to the magnitude of increase in peak responses ($r = 0.19$, $P = 0.22$, Fig. 6). The difference in the changes of the RF width induced by bicuculline was not likely due to the difference in the amount of applied bicuculline.

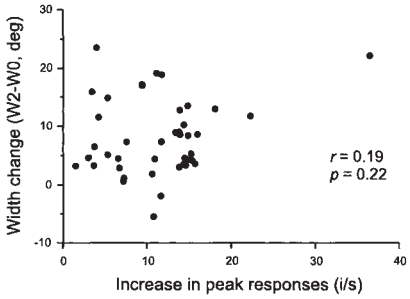


**Figure 6.** The change in the RF width induced following bicuculline application is not correlated with the increased responses at the original peak. The difference in widths (*y*-axis) between during (W2) and before bicuculline application (W0) in the RF tuning curves of a neuron, measured at the original half-peak level, was plotted against the difference in responses of the neuron between during and before bicuculline application at the original peak (*x*-axis). Pearson's correlation coefficients (*r*) and *P* values are shown inside ($n = 43$).

### *Stimulus-dependency of Bicuculline Effects*

We have previously shown that the effect of bicuculline on the responses of TE neurons at the RF center depends on stimuli (Wang *et al.*, 2000). In the present study, we show that the effect of bicuculline is stimulus-dependent also at the peripheral region of the RF. Figure 7 shows an example of a neuron. The RF response profile of this neuron to one stimulus, a gradation pattern, was significantly affected by bicuculline (two-ANOVA, $P < 0.05$, Fig. 7*A*). In contrast, the RF response profiles to a gradation pattern of the opposite gradient (Fig. 7*B*) and to another luminance pattern (Fig. 7*C*) were not affected (two-ANOVA, $P > 0.05$), although the two stimuli were also effective before bicuculline application. Responses of this neuron at the RF center to the stimulus in Figure 7*A* during bicuculline application were higher than those to the most effective stimulus before bicuculline application (Fig. 7*B*). The failure to enhance the responses to the stimuli shown in Figure 7*B*,*C* is thus not due to saturation of firing rate in this neuron. Seven of 38 neurons tested in the five-location or seven-location experiments exhibited this kind of stimulus-specific disinhibition. Bicuculline only affected responses of these neurons to a portion of stimuli. A relatively small number of neurons showed this kind of effects compared to our previous results on the responses at the RF

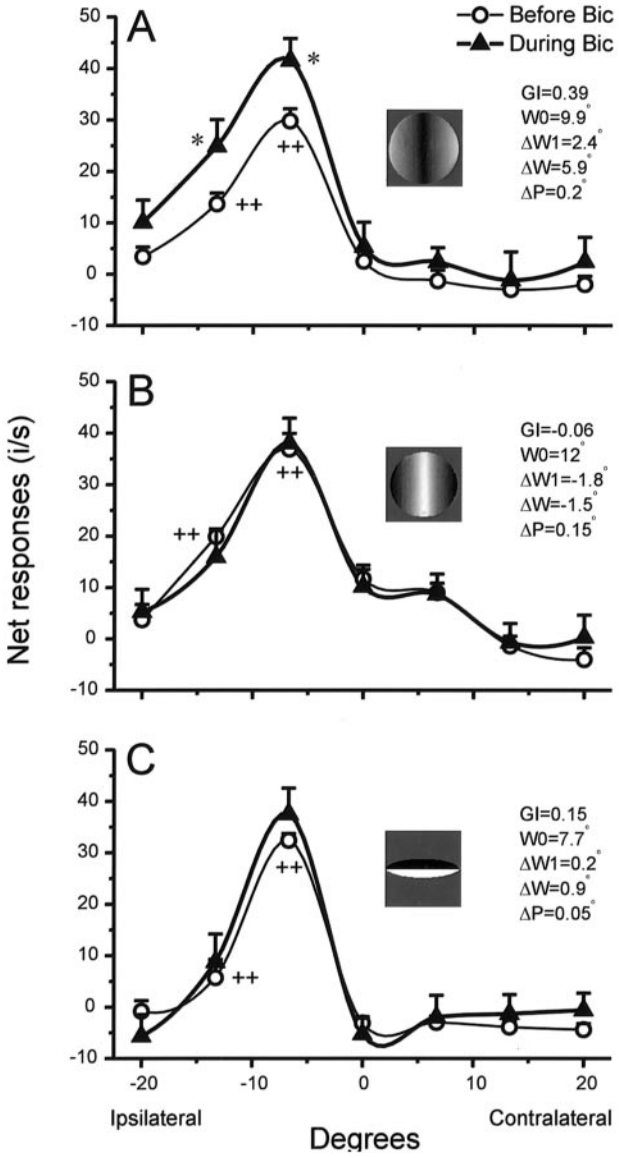


**Figure 7.** Stimulus-specific disinhibitory effects of bicuculline in a TE neuron. (*A–C*) RF tuning curves obtained with three different stimuli. The RF response profile to one originally effective stimulus (*A*) was affected by bicuculline (two-ANOVA, $P < 0.05$), but the RF response profiles to two other effective stimuli (*B*,*C*) were not affected ($P > 0.05$). Note that the stimulus in (*B*) was the most effective one before bicuculline application and that responses at the RF center to the stimulus (*A*) during bicuculline were larger than responses to the most effective stimulus (*B*). For other conventions, see Figures 1 and 4.

center (Wang *et al.*, 2000). This is probably because the number of stimuli tested for each neuron was small (three) in the present experiments.

In order to evaluate the stimulus dependency of bicuculline effects on the RF, a three-way ANOVA with stimulus, location and drug as factors was performed for each neuron tested (Table 1). When effects of bicuculline were examined across all the stimuli used for a neuron, visual responses of 71% (27/38) of neurons were significantly affected by bicuculline application (Drug factor, $P < 0.05$, third column of Table 1). The percentage was lower than that obtained when a two-way ANOVA was applied to each stimulus (95%, 36/38, see above and Materials and Methods). This is because, for nine neurons of the 36

**Table 1**
Effects of bicuculline on visual responses of TE neurons to stimuli presented across RFs

| Three-way ANOVA | Factors ($P < 0.05$) | | | Interactions ($P < 0.05$) | | | |
|---|---|---|---|---|---|---|---|
| | Stim | Loc | Drug | Stim × Loc | Loc × Drug | Stim × Drug | Stim × Loc × Drug |
| Five-location experiment ($n = 17$) | 17 | 16 | 12 | 12 | 9 | 13 | 3 |
| Seven-location experiment ($n = 21$) | 21 | 21 | 15 | 15 | 13 | 11 | 2 |
| Total neurons | 38 | 37 | 27 | 27 | 22 | 24 | 5 |
| Percentage (%)[a] | 100 | 97 | 71 | 71 | 58 | 63 | 13 |

[a]Of the 38 neurons tested in the five- and seven-location experiments. Stim, stimulus; Loc, location.

neurons showing bicuculline effects in the two-way ANOVA test, one or two of the three stimuli used were ineffective even during the application of bicuculline, or one or two stimuli were effective before the bicuculline application but the responses to them were not affected by bicuculline (e.g. the neuron in Fig. 7). A significant interaction between stimulus and bicuculline was observed in 63% (24/38) of neurons (Stimulus × Drug interaction, $P < 0.05$, sixth column of Table 1), suggesting that bicuculline effects on an RF are dependent on stimuli in these neurons across the stimulated locations. In 58% (22/38) of neurons, the effects of bicuculline were dependent on the stimulated location (Location × Drug interaction, $P < 0.05$, fifth column of Table 1). The results indicate that these neurons received spatially specific inhibitory inputs; the distribution of inhibitory inputs is different across the stimulus locations but is similar among the stimuli used. Finally, a significant interaction among stimulus, location and bicuculline occurred in 13% of neurons (5/38, Stimulus × Location × Drug interaction, $P < 0.05$, seventh column of Table 1). In these neurons, bicuculline caused different changes in RF structures when the RFs were tested with different stimuli. This suggests that this population of neurons received spatially specific inhibitory inputs derived from different stimuli. The fractions of the latter three groups of neuron are likely to be an underestimate, because only a small number of stimuli was used in these experiments.

These results indicate that the disihibitory effects of bicuculline on the RF cannot be explained simply by a general increase in excitability of neurons. The effects are dependent on the excitatory inputs of the stimuli that were under the influence of GABAergic inhibition.

### *Silenced Excitatory Inputs throughout RF*

We have previously shown that many TE neurons under blockade of inhibition begin to respond to originally ineffective stimuli presented at the center of RFs (Wang *et al.*, 2000). Similar phenomena occurred also in the peripheral regions of the RFs. The neuron shown in Figure 8*A*, for instance, originally did not respond to a pattern composed of a yellow circle and a green star (S1) at all the tested locations. Following the application of bicuculline, it responded to the pattern presented at the RF center and three of the four peripheral locations (5.3°). The neuron also began to respond to an image of the bottom view of a tomato (S2) presented at four surrounding locations (5.3°). This neuron originally showed no responses at these locations and only weak responses at the center. By contrast, this neuron responded to another stimulus, the side view of a peach, at all the five locations under control conditions, and enhanced its responses at three surrounding locations during bicuculline application.

Three of the 16 neurons tested in the five-location experi-

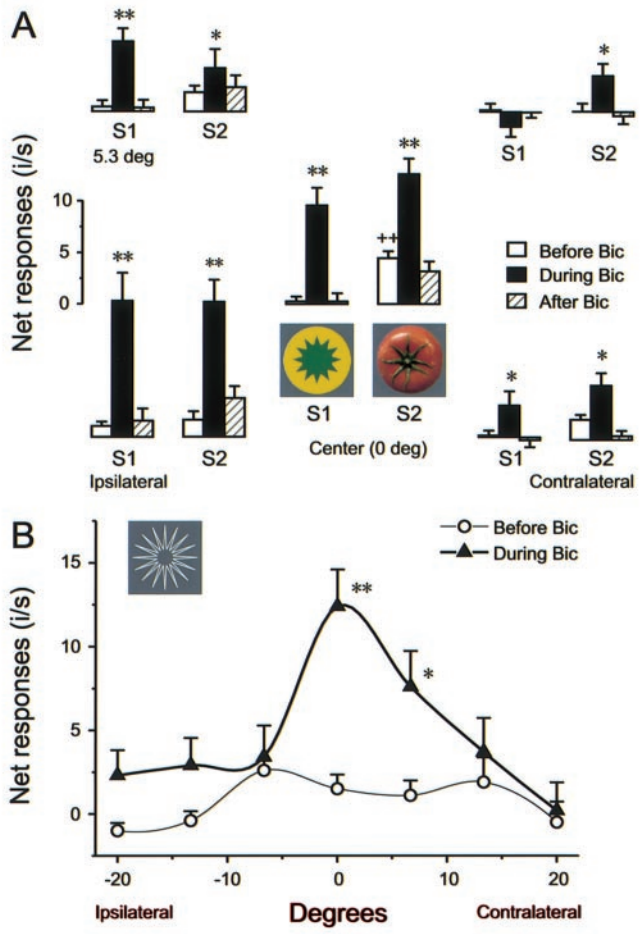


**Figure 8.** Inputs of originally ineffective stimuli existed throughout the RF. (*A*) Net responses of a neuron to stimulus 1 (S1) and stimulus 2 (S2) tested at the RF center and four surrounding locations before (open bars), during (filled bars) and after (hatched bars) bicuculline application. (*B*) RF tuning curves of another neuron examined at seven horizontally separated locations. ++, $P < 0.01$, *t*-test, relative to the spontaneous firing rate **, *, $P < 0.01$ or 0.05, *t*-test for comparing net responses during bicuculline application with those before bicuculline application. Vertical bars: SEM. For other conventions, see Figures 1, 3 and 4.

ments exhibited a similar behavior to one originally ineffective stimulus, and another neuron to two originally ineffective stimuli. Similar effects were observed in two of the 20 neurons tested at seven locations; an example is shown in Figure 8*B*. Because the number of stimuli used in the present experiments was small (three stimuli) and we selected effective stimuli whenever possible, the proportion of neurons that showed this behavior was much lower (17%, 6/36) than that reported in our previous study (84%) on the responses at the RF center (Wang *et al.*, 2000). The results indicate that excitatory inputs masked by GABAergic inhibition under normal conditions exist in the RF periphery as well as at the RF center.

### *Excitatory and Inhibitory Input in the Surrounding Regions*

Most RFs (84%, 36/43) had no obvious change in the position of the response peak (≤2°, Fig. 9) following bicuculline application and the strongest responses remained at the original RF center (e.g. Fig. 4*A–D*). This indicates that excitatory inputs to most neurons were strongest at the center of their RFs with or without GABAergic inhibition.

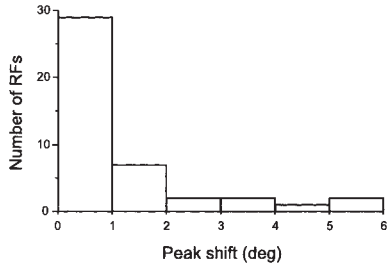


**Figure 9.** Distribution of the shift in the peak position of RF tuning curves ($n = 43$) before and during bicuculline application.

However, some neurons showed the largest disinhibition at the RF periphery (e.g. Fig. 4*D,E*). The disinhibition in the surrounding regions shifted the response peak of 16% (7/43) of the RFs from the original location by >2° (Figs 4*E* and 9). In these neurons, a GABAergic inhibitory input predominant in the surrounding regions generates their RF profiles under normal conditions.

### *'Hole' without Input within RFs*

One neuron had a 'hole' within the RF where visual inputs of some stimuli effective at adjacent regions did not appear to reach. The neuron shown in Figure 10 did not respond to a stimulus, a half-white and half-black ellipse, presented at position 3 (–6.7°), whereas it exhibited clear visual responses to the same stimulus presented at both sides of this location (positions 2 and 4) under normal conditions (Fig. 10*A*). Bicuculline application enhanced its responses to the stimulus at positions 2 and 4, but not at position 3 (Fig. 10*A*). The results suggest that the neuron did not receive input of the stimulus feature at this local region within its RF. Responses of the neuron to the second stimulus, a gradation pattern, under normal conditions were similar to those to the first stimulus (Fig. 10*B*). Following bicuculline application, however, the stimulus elicited responses of the neuron at position 3. Thus, the neuron received inputs of the second stimulus at this location that were silenced by GABAergic inhibition under normal conditions. Importantly, the third stimulus, another gradation pattern, at the location activated this neuron (Fig. 10*C*) under normal conditions, indicating that the absence of responses to the first stimulus was not attributable to a deficit in the retina. Indeed, we did not detect any abnormalities in the retina by observing the fundus of both eyes with a retinal camera and an ophthalmoscope. Afferent information on the stimulus feature shown in Figure 10*A* thus did not completely cover the entire RF in this neuron. The size of this silent 'hole' was at least 3° (size of a stimulus and its movement magnitude, 2.5° + 0.5°).

The same neuron did not respond to all three stimuli presented at position 6 under both normal and disinhibited conditions ($P > 0.05$). The RF center of the neuron was a few degrees contralateral to the fovea. Retinoscopic examination showed that the optic disc of the retina was 15.8° from the fovea on the contralateral side. Given that the distance of the silent region at position 6 was 13.3° from the RF center, the region should correspond to the 'blind spot' or the local visual field corresponding to the optic disc of the retina where there are no photoreceptors.

The response behaviors of this neuron to the three different stimuli presented inside the silent 'hole' and the 'blind spot' indicate that the differences between the responses of neurons to the different stimuli during bicuculline application are related to whether there exist excitatory inputs of the stimulus features

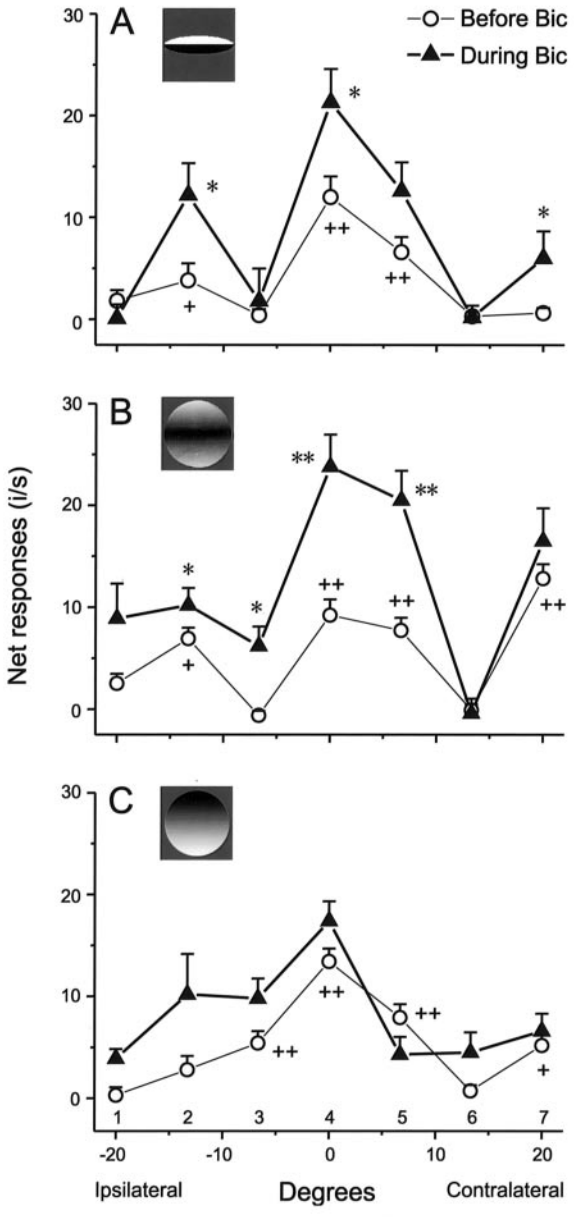


**Figure 10.** RF tuning curves obtained with three different stimuli (insets) of a neuron with a region lacking excitatory inputs of a stimulus feature (*A*) within its RF. The region was located at the ipsilateral side 6.7° (position 3) from the RF center. The neuron also had the 'blind spot' within its RF at the contralateral side 13.3° (position 6) from the center, where none of the three stimuli evoked responses before and during bicuculline application. For other conventions, see Figures 1 and 4.

at a location of RFs and to whether the excitatory inputs are under GABAergic inhibition, rather than to stochastic fluctuations in responses induced by blockade of GABAergic synapses.

## Discussion

The present experiments showed that: (i) removal of $GABA_A$-receptor-mediated inhibition enhanced visual responses of TE neurons at the periphery of or outside RFs, as well as at the center of RFs, thus resulting in enlargement of RFs of many TE neurons; (ii) the largest disinhibition usually occurred at the RF center, but some neurons had the strongest inhibitory input in the periphery; and (iii) stimulus inputs completely suppressed by GABAergic inhibition existed not only at the RF center, but throughout the RF. The results suggest that GABAergic inhibition plays a crucial role in the construction of normal RF structures in TE neurons.

In addition, the study provided a quantitative measure of the size of normal RFs of TE neurons by presenting stimuli at seven locations along the horizontal dimension across 40°. As a recent study reported (De Beeck and Vogels, 2000), most of the RFs had a bell-shaped profile with the most sensitive region located at the central portion, and the RF size considerably varied among TE neurons. The width measured at the half-peak level of RF tuning curves was 15.4 ± 6.9°. Although an effective stimulus usually evoked responses throughout an RF, we found a neuron that had a 'hole' within its RF where inputs of some stimulus features effective at adjacent stimulus locations did not reach. This suggests that the convergence of inputs from earlier areas in the cortical hierarchy is not necessarily complete throughout the RF.

### *Technical Consideration*

A detailed methodological consideration on the application of bicuculline has been given elsewhere (Fujita and Konishi, 1991). Here we discuss two technical points that we did not address previously. The first concerns the size of the volume affected by iontophoresed bicuculline. Although we did not attempt to determine experimentally the extent of bicuculline diffusion, the effective diffusion distances of iontophoretically applied dopamine, penicillin and D-2-amino-5-phosphonovaleric acid (APV, a glutamate receptor antagonist) in brain tissues have been reported by several research groups. The effective diffusion distance of APV is estimated to be 100–200 μm from the site of iontophoresis in the cat visual cortex (Fox *et al.*, 1989). Diffusion dynamics analysis indicates that the effective action range of dopamine and penicillin is within a radius of ~150 μm from the site of iontophoresis (Lehmenkühler *et al.*, 1991; Nicholson, 1995).

The diffusion distance of bicuculline in the present study is likely to be <100–200 μm, because the mol. wt of bicuculline (509.3) is larger than that of APV (197.1), dopamine (153.1) and penicillin (149.2), and because we used a small pipette tip (2–4 μm in diameter) and a low ejecting current (+1 to 5 nA). The spherical cortical region in the radius of ~150 μm contains 600–800 neurons (Rockel *et al.*, 1980; Lehmenkühler *et al.*, 1991). Most likely bicuculline affected not only the recorded single neuron, but also a group of nearby neurons.

Bicuculline could also exert network effects on the observed neurons from distant neurons within area TE via long-range horizontal axons (Fujita and Fujita, 1996) and from neurons in afferent areas via feedforward and feedback processes. Inactivation of the local inhibitory circuit around the site of iontophoresis could facilitate these mutual excitatory inputs, either by disinhibiting nearby neurons, in turn facilitating the recorded neuron, or by disinhibiting the recorded neuron, then facilitating nearby neurons, distant neurons within area TE or in afferent areas, and affecting the recorded neuron again via a re-entering process. All these effects are, however, due to the removal of the local GABAergic inhibition around the recorded neuron.

The second technical issue concerns the use of balance currents. The balance currents may induce an uptake of bicuculline into the vehicle barrel during the long ejection period and the bicuculline would be released from the barrel once the current was switched to the retaining current with a comparatively high intensity and the opposite polarity. This is theoretically possible, but is unlikely to be a practical problem. In the present experiments, we used low ejection currents of +1 to +5 nA

which expelled a minimal amount of bicuculline. The balance currents with the same intensity and opposite polarity may induce an uptake of a small proportion of the ejected bicuculline into the vehicle barrel. Note that the expelled bicuculline would be diluted in extracellular space and would be diluted again with 0.9% NaCl if it was taken up into the vehicle barrel. When the polarity of the current was switched, the high retaining current of +20 nA from the vehicle barrel would quickly drive out this microamount of bicuculline. Usually, we collected the recovery data at least 5–10 min after the polarity of the current was switched. During this period, bicuculline should have been diffused. We believe that what is described above is likely the case, because almost all neurons in the present experiments and 89% of neurons in the previous study (Wang *et al.*, 2000) restored their responses to the original level after the application of bicuculline was stopped.

### *Construction of RF Structure and Selectivity of TE Neurons*

Blockade of GABAergic inhibition enlarged RFs of most of the TE neurons. The shape of the RF tuning curve, however, did not change in the presence of bicuculline in 44% of the tested RFs (Figs 4*B* and 5*D*), suggesting a simple gain control of visual responses by GABAergic inhibition in these neurons. In the other 56% of the RFs, the shape of the RF tuning curve was altered by bicuculline (Fig. 5*D*). The effects could be explained by some specific interactions between neurons. If interconnected neurons have RFs with different sizes but with their RF centers at similar retinotopic positions, the removal of inhibitory inputs from neurons with large RFs would result in the RF shape of postsynaptic neurons becoming broader (35% RFs), whereas the removal of inhibition from neurons with small RFs would result in the RF shape of postsynaptic neurons becoming sharper (21% RFs). Some neurons had strong excitatory inputs at a peripheral region in the RF, which were partially masked by inhibition (Figs 4*D*,*E* and 10*A*,*B*). These excitatory inputs at sites off from the RF center may arise from other TE neurons having RF centers at different retinotopic locations or from neurons at different retinotopic regions of earlier cortical areas TEO or V4.

A previous study suggested that the selectivity of neurons for object features is generated in areas V4 and TEO, and transferred to area TE (Kobatake and Tanaka, 1994). The response selectivity for a particular feature with invariance of the stimulus position is hypothesized to be generated by convergent projections from neurons having the same stimulus selectivity but with different RF positions in these earlier areas. The hypothesis needs two prerequisites. First, each local retinotopic region in the afferent areas must contain a set of neurons selective for different object features that are represented in area TE. Second, each neuron in area TE must receive convergent projections of the same feature from all different retinotopic sites of its afferent areas.

Our previous study has shown that a substantial fraction of excitatory inputs to TE neurons at the RF center is masked by GABAergic inhibition (Wang *et al.*, 2000). The marked enlargement of RFs of TE neurons induced by bicuculline in the present study indicates that visual information converges upon TE neurons from wider retinotopic regions beyond their normal RFs. If each TE neuron or a population of neurons in a columnar region (Fujita *et al.*, 1992) receives such projections specific for a stimulus feature but converging from a wide visuotopic area, the wiring between the afferent cortical areas and TE would be massive. An anatomical study has, however, shown that axons from a local region in area TEO terminate in only a few multiple columnar regions of 200–300 μm in width in area TE, not in broadly divergent regions of area TE (Saleem *et al.*, 1993).

At the RF center, TE neurons receive multiple, heterogeneous stimulus inputs, some of which are masked by GABAergic inhibition, and the stimulus features of the masked inputs are related to those of the originally effective stimuli for these neurons or for nearby neurons (Wang *et al.*, 2000). The present results indicate that the masked inputs exist not only at the RF center, but also throughout the entire RF. These inputs to the entire RF must also be involved in constructing the RF structures and selectivity of TE neurons.

The distinctive response behaviors of the neuron shown in Figure 10 to the three stimuli at position 3 under normal and disinhibited conditions suggest that inputs of the three stimulus features have different projections to the RF in this local region. In addition, the response patterns of the neuron in Figure 8*A* indicate that the distributions of the excitatory inputs of two analogous stimuli are shifted with respect to each other and have different gravity centers of projections within the RF. Thus, afferent inputs converging to individual TE neurons from different retinotopic sites do not necessarily possess the same feature and may have different projection distributions within the RF of a TE neuron. The convergence of afferent inputs is also not necessarily complete throughout the RF (Fig. 10). The present results give rise to a scheme different from that proposed by Kobatake and Tanaka (Kobatake and Tanaka, 1994). We propose that the generation of the feature selectivity and the large RF of TE neurons is accomplished in area TE both by the convergent processes of afferent inputs and by excitatory and inhibitory interactions mediated by neuronal circuits within area TE. This scheme is different from that of Kobatake and Tanaka (Kobatake and Tanaka, 1994) in three respects. First, the construction of feature selectivity of TE neurons continues within area TE (Wang *et al.*, 2000). Second, afferent inputs converging to a TE neuron can convey heterogeneous stimulus features (Wang *et al.*, 2000). Third, afferent inputs may have different projection distributions within the RF of a TE neuron.

### *Source of GABAergic Inhibition*

There are three possible sources for the GABAergic inhibition we observed in this study. The first one is a short-range inhibition driven by excitatory, recurrent inputs of local pyramidal neurons. The second is a 'long-range' inhibition within area TE. Because axons of most GABAergic interneurons so far identified in area TE (Tanigawa *et al.*, 1998) project horizontally only in a range <1 mm, this type of inhibition is mostly driven by long-range excitatory horizontal axons of pyramidal neurons at distant sites within area TE. GABAergic inhibition driven by excitatory glutamatergic synapses of long-range connections has been demonstrated in the ferret area 17 (Weliky *et al.*, 1995). Large basket cells in cat areas 17 and 18 project their horizontal axons up to a distance of 3.8 mm (Somogyi *et al.*, 1983; Kisvárday and Eysel, 1993; Kisvárday *et al.*, 1993). They receive intracortical inputs from pyramidal cells or other large basket cells and afferent excitatory inputs from early areas (Somogyi *et al.*, 1983; Kisvárday *et al.*, 1993; Kisvárday and Eysel, 1993). Their counterparts in area TE, although not demonstrated yet, may also be engaged in this long-range inhibitory process. The third one is a 'long-range' inhibition from afferent areas TEO and V4. This inhibition is driven most likely by long-range excitatory projections from these afferent areas to area TE, as those from area 17 to area 18 of the rat visual cortex (Johnson and Burkhalter, 1996; Shao and Burkhalter, 1996; Gonchar and Burkhalter, 1999). It is unknown whether a 'direct' long-range

inhibitory projection from areas TEO and V4 to area TE exists, as the direct long-range projection of inhibitory neurons between area 17 and area 18 in the rat visual cortex (McDonald and Burkhalter, 1993).

### *GABAergic Contribution to Generating RF Structures in Other Cortices*

GABAergic inhibition participates in generating RF structures of the primary visual cortical neurons. Blockade of GABAergic inhibition by iontophoretic application of bicuculline changes RF structures of neurons in the cat visual areas 17 and 18 (Sillito, 1975, 1977; Sillito and Versiani, 1977; Wolf *et al*., 1986; Eysel *et al.*, 1994; Eysel and Shevelev, 1998; Pernberg *et al*., 1998; Murthy and Humphrey, 1999; Frégnac and Shulz, 1999). During bicuculline application, On and Off subfields of RFs of simple cells in space and time and those of complex cells in time become more overlapping with each other. Thus, simple cells, at least outside layer IV, receive both On and Off excitatory inputs across most parts of the RFs, which are similar to the excitatory On and Off inputs of the kind found in complex cells. The spatial specificity of intracortical inhibition is suggested to contribute to spatially isolated On and Off subfields in simple cells (Frégnac and Shulz, 1999). Shunting inhibition mediated by $GABA_A$ receptors is involved in the separation of On and Off subfields of simple cells and the mixed On/Off field of complex cells (Borg-Graham *et al*. 1998). GABAergic inhibition is also involved in response selectivity of cat area 17 neurons for cross-like patterns (Shevelev *et al*., 1998) and On/Off response characteristics of color-selective neurons in macaque V1 (Sato *et al*., 1994).

The contribution of GABAergic inhibition to the spatial receptive field is not limited to the visual cortex. Blockade of GABAergic inhibition by bicuculline changes the size, structure and response properties of RFs of neurons in a variety of cortical areas such as the rat barrel cortex (Kyriazi *et al*., 1996), the cat and macaque primary somatosensory cortex (Dykes *et al*., 1984; Alloway *et al*., 1989; Alloway and Burton, 1991), the macaque prefrontal cortex (Rao *et al*., 2000) and the rat primary motor cortex (Jacobs and Donoghue, 1991).

Neurons in the visual and somatosensory cortex expand their RFs after lesions of afferent areas, deprivation or abnormal experience of sensory inputs, artificial scotoma, and their RFs are also dependent on the synchronized state of the electroencephalogram under anesthesia and contextual stimulus-contrast under awake conditions (Gilbert, 1998; Wörgötter *et al*., 1998; Kapadia *et al*., 1999; Polley *et al*., 1999). RF size of cortical neurons is thus not fixed and can vary in a dynamic manner. GABAergic inhibition may be engaged in some aspects of the dynamic regulation of RFs of cortical neurons.

## Conclusions

The RF and stimulus selectivity of TE neurons are generated by integrating information of multiple inputs originating from a wide retinotopic region beyond their normal RF. These inputs are not necessarily similar to each other in the stimulus feature information they convey and may have distinctive projection distributions within the RF of a TE neuron. The afferent convergence is not necessarily complete throughout a RF. Intrinsic GABAergic inhibition is critically involved in the construction of the normal RF structures and feature selectivity of TE neurons from these inputs.

## Notes

We thank John Maunsell for his comments on the manuscript. Magnetic resonance images were taken at the National Institute for Physiological Sciences. This work was supported by a CREST grant from the Japan Science and Technology Corporation and grants from the Japanese Ministry of Education, Science, Sports and Culture (to I.F.). In the earlier stages of this work, Y.W. was supported by a fellowship from the Uehara Memorial Foundation and Y.M. by a fellowship from the Japan Society for the Promotion of Science for Young Scientists.

Address correspondence to Ichiro Fujita, Laboratory for Cognitive Neuroscience, Division of Biophysical Engineering, Graduate School of Engineering Science, Osaka University, 1–3 Machikaneyama, Toyonaka, Osaka 565-8531, Japan. Email: fujita@bpe.es.osaka-u.ac.jp.

## References

Alloway KD, Burton H (1991) Differential effects of GABA and bicuculline on rapidly- and slowly-adapting neurons in primary somatosensory cortex of primates. Exp Brain Res 85:598–610.

Alloway KD, Rosenthal P, Burton H (1989) Quantitative measurements of receptive field changes during antagonism of GABAergic transmission in primary somatosensory cortex of cats. Exp Brain Res 78:514–532.

Borg-Graham LJ, Monier C, Frégnac Y (1998) Visual input evokes transient and strong shunting inhibition in visual cortical neurons. Nature 393:369–373.

Boussaoud D, Desimone R, Ungerleider LG (1991) Visual topography of area TEO in the macaque. J Comp Neurol 306:554–575.

De Beeck OP, Vogels R (2000) Spatial sensitivity of macaque inferior temporal neurons. J Comp Neurol 426:505–518.

Desimone R, Gross CG (1979) Visual areas in the temporal cortex of the macaque. Brain Res 178:363–380.

Desimone R, Albright TD, Gross CG, Bruce C (1984) Stimulus-selective properties of inferior temporal neurons in the macaque. J Neurosci 4:2051–2062.

Dykes RW, Landry P, Metherate R, Hicks TP (1984) Functional role of GABA in cat primary somatosensory cortex: shaping receptive fields of cortical neurons. J Neurophysiol 52:1066–1093.

Eysel UT, Shevelev IA (1998) Orientation tuning and receptive field structure in cat striate neurons during local blockade of intracortical inhibition. Neuroscience 84:25–36.

Eysel UT, Shevelev IA, Lazareva NA, Sheraev GA (1994) Time-slice analysis of inhibition in cat striate cortical neurones. NeuroReport 5:2033–2036.

Fox K, Sato H, Daw N (1989) The location and function of NMDA receptors in cat and kitten visual cortex. J Neurosci 9:2443–2454.

Frégnac Y, Shulz DE (1999) Activity-dependent regulation of receptive field properties of cat area 17 by supervised Hebbian learning. J Neurobiol 41:69–82.

Fujita I, Fujita T (1996) Intrinsic connections in the macaque inferior temporal cortex. J Comp Neurol 368:467–486.

Fujita I, Konishi M (1991) The role of GABAergic inhibition in processing of interaural time difference in the owl's auditory system. J Neurosci 11:722–739.

Fujita I, Tanaka K, Ito M, Cheng K (1992) Columns for visual features of objects in monkey inferotemporal cortex. Nature 360:342–346.

Gattass R, Gross CG, Sandell JH (1981) Visual topography of V2 in the macaque. J Comp Neurol 201:519–539.

Gattass R, Sousa APB, Gross CG (1988) Visuotopic organization and extent of V3 and V4 of the macaque. J Neurosci 8:1831–1856.

Gilbert CD (1998) Adult cortical dynamics. Physiol Rev 78:467–485.

Gonchar Y, Burkhalter A (1999) Differential subcellular localization of forward and feedback interareal inputs to parvalbumin expressing GABAergic neurons in rat visual cortex. J Comp Neurol 406:346–360.

Goodale MA, Milner AD (1992) Separate visual pathways for perception and action. Trends Neurosci 15:20–25.

Gross CG, Mishkin M (1977) The neural basis of stimulus equivalence across retinal translation. In: Lateralization in the nervous system (Harnad S, Doty R, Jaynes J, Goldstein L, Krauthamer G, eds), pp. 109–122. New York: Academic Press.

Gross CG, Rocha-Miranda CE, Bender DB (1972) Visual properties of neurons in inferotemporal cortex of the macaque. J Neurophysiol 35:96–111.

Hendry SHC, Schwark HD, Jones EG, Yan J (1987) Number and proportions of GABA-immunoreactive neurons in different areas of monkey cerebral cortex. J Neurosci 7:1503–1519.

Hubel DH, Wiesel TN (1974) Uniformity of monkey striate cortex: a

parallel relationship between field size, scatter, and magnification factor. J Comp Neurol 158:295–302.
Ito M, Tamura H, Fujita I, Tanaka K (1995) Size and position invariance of neuronal responses in monkey inferotemporal cortex. J Neurophysiol 73:218–226.
Jacobs KM, Donoghue JP (1991) Reshaping the cortical motor map by unmasking latent intracortical connections. Science 251:944–947.
Johnson RR, Burkhalter A (1996) Microcircuitry of forward and feedback connections within rat visual cortex. J Comp Neurol 368:383–398.
Kapadia MK, Westheimer G, Gibert CD (1999) Dynamics of spatial summation in primary visual cortex of alter monkeys. Proc Natl Acad Sci USA 96:12073–12078.
Kisvárday ZF, Eysel UT (1993) Functional and structural topography of horizontal inhibitory connections in cat visual cortex. Eur J Neurosci 15:1558–1572.
Kisvárday ZF, Beaulieu C, Eysel UT (1993) Network of GABAergic large basket cells in cat visual cortex (area 18): implication for lateral disinhibition. J Comp Neurol 327:398–415.
Kobatake E, Tanaka K (1994) Neuronal selectivities to complex object features in the ventral visual pathway of the macaque cerebral cortex. J Neurophysiol 71:856–867.
Kyriazi HT, Carvell GE, Brumberg JC, Simons DJ (1996) Quantitative effects of GABA and bicuculline methiodide on receptive field properties of neurons in real and simulated whisker barrels. J Neurophysiol 75:547–560.
Lehmenkühler A, Nicholson C, Speckmann EJ (1991) Threshold extracellular concentration distribution of penicillin for generation of epileptic focus measured by diffusion analysis. Brain Res 561: 292–298.
Lueschow A, Miller EK, Desimone R (1994) Inferior temporal mechanisms for invariant object recognition. Cereb Cortex 5:523–531.
McDonald CT, Burkhalter A (1993) Organization of long-range inhibitory connections within rat visual cortex. 13:768–781.
Miller EK, Gochin PM, Gross CG (1991) Habituation-like decrease in the responses of neurons in inferior temporal cortex of the macaque. Vis Neurosci 7:357–362.
Murthy A, Humphrey AL (1999) Inhibitory contributions to spatiotemporal receptive-field structure and direction selectivity in simple cells of cat area 17. J Neurophysiol 81:1212–1224.
Nicholson C (1995) Interaction between diffusion and Michaelis–Menten uptake of dopamine after iontophoresis in striatum. Biophys J 68:1699–1715.
Pernberg J, Jirmann K, Eysel UT (1998) Structure and dynamics of receptive fields in the visual cortex of the cat (area 18) and the influence of GABAergic inhibition. Eur J Neurosci 10:3596–3606.
Polley DB, Chen-Bee CH, Frostig RD (1999) Two directions of plasticity in the sensory-deprived adult cortex. Neuron 24:623–637.
Rao SG, Williams GV, Goldman-Rakic P (2000) Destruction and creation of spatial tuning by disinhibition: $GABA_A$ blockade of prefrontal cortical neurons engaged by working memory. J Neurosci 20: 485–494.
Rockel AJ, Hiorns RW, Powell TPS (1980) The basic uniformity in structure of the neocortex. Brain 103:221–244.
Saleem KS, Tanaka K, Rockland KS (1993) Specific and columnar projection from area TEO to TE in the macaque inferotemporal cortex. Cereb Cortex 3:454–464.
Sato H, Katsuyama N, Tamura H, Hata Y, Tsumoto T (1994) Broad-tuned chromatic inputs to color-selective neurons in the monkey visual cortex. J Neurophysiol 72:163–168.
Sato H, Katsuyama N, Tamura H, Hata Y, Tsumoto T (1995) Mechanisms underlying direction selectivity of neurons in the primary visual cortex of the macaque. J Neurophysiol 74:1382–1394.
Sato H, Katsuyama N, Tamura H, Hata Y, Tsumoto T (1996) Mechanisms underlying orientation selectivity of neurons in the primary visual cortex of the macaque. J Physiol 494:757–771.
Schwartz EL, Desimone R, Albright TD, Gross CG (1983) Shape recognition and inferior temporal neurons. Proc Natl Acad Sci USA 80:5776–5778.
Seacord L, Gross CG, Mishikin M (1979) Role of inferior temporal cortex in interhemispheric transfer. Brain Res 167:259–272.
Shao Z, Burkhalter A (1996) Different balance of excitation and inhibition in forward and feedback circuits of rat visual cortex. J Neurosci 16:7353–7365.
Shevelev IA, Jirmann KU, Sharaev GA, Eysel UT (1998) Contribution of GABAergic inhibition to sensitivity to cross-like figures in striate cortex. NeuroReport 9:3153–3157.
Sillito AM (1975) The contribution of inhibitory mechanisms to receptive field properties of neurones in the striate cortex of the cat. J Physiol (Lond) 250:305–329.
Sillito AM (1977) Inhibitory processes underlying the direction specificity of simple, complex, and hypercomplex cells in the cat's visual cortex. J Physiol (Lond) 271:699–720.
Sillito AM, Versiani V (1977) The contribution of excitatory and inhibitory inputs to the length preference of hypercomplex cells in layers II and III of the cat's striate cortex. J Physiol (Lond) 273:775–790.
Somogyi P, Kisvárday ZF, Martin KAC, Whitteridge D (1983) Synaptic connections of morphologically identified and physiologically characterized large basket cells in the striate cortex of cat. Neuroscience 10:261–294.
Takao M, Wang Y, Miyoshi T, Fujita I, Fukuda Y (2000) A new intraretinal recording system with multiple-barreled electrodes for pharmacological studies on cat retinal ganglion cells. J Neurosci Meth 97:87–92.
Tanaka K, Saito H-A, Fukada Y, Moriya M (1991) Coding visual images of objects in the inferotemporal cortex of the macaque monkey. J Neurophysiol 66:170–189.
Tanigawa H, Fujita I, Kato M, Ojima H (1998) Distribution, morphology, and γ-aminobutyric acid immunoreactivity of horizontally projecting neurons in the macaque inferior temporal cortex. J Comp Neurol 401:129–143.
Tovee MJ, Rolls ET, Azzopardi P (1994) Translation invariance in the responses to faces of single neurons in the temporal visual cortical areas of the alert macaque. J Neurophysiol 72:1049–1060.
Tsumoto T, Eckart W, Creutzfeldt OD (1979) Modification of orientation sensitivity of cat visual cortex neurons by removal of GABA-mediated inhibition. Exp Brain Res 34:351–363.
Ungerleider LG, Mishkin M (1982) Two cortical visual systems. In: The analysis of visual behavior (Ingle DJ, Mansfield RJW, Goodale MA, eds), pp. 549–586. Cambridge, MA: MIT Press.
Wang Y, Fujita I, Murayama Y (2000) Neuronal mechanisms of selectivity for object features revealed by blocking inhibition in inferotemporal cortex. Nature Neurosci 3:807–813.
Weliky M, Kandler K, Fitzpatrick D, Katz LC (1995) Patterns of excitation and inhibition evoked by horizontal connections in visual cortex share a common relationship to orientation columns. Neuron 15:541–552.
Wolf W, Hicks TP, Albus K (1986) The contribution of GABA-mediated inhibitory mechanisms to visual response properties of neurons in the kitten's striate cortex. J Neurosci 6:2779–2795.
Wörgötter F, Suder K, Zhao Y, Kerscher N, Eysel UT, Funke K (1998) State-dependent receptive-field restructuring in the visual cortex. Nature 396:165–168.